Journal of Magnetic Resonance 194 (2008) 67–75

Contents lists available at ScienceDirect

Journal of Magnetic Resonance

journal homepage: www.elsevier.com/locate/jmr

Synthetic signal injection using inductive coupling

Kenneth I. Marro [a,*,1], Donghoon Lee [a,1], Eric G. Shankland [a], Clinton M. Mathis [a], Cecil E. Hayes [a], Catherine E. Amara [c], Martin J. Kushmerick [a,b]

[a] Department of Radiology, University of Washington, 1959 NE Pacific Street, Box 357115, Seattle, WA 98195-7115, USA
[b] Department of Physiology and Biophysics, University of Washington, Seattle, WA, USA
[c] Faculty of Physical Education and Health, University of Toronto, Toronto, Ont., Canada

ARTICLE INFO

Article history:
Received 26 March 2008
Revised 15 May 2008
Available online 1 July 2008

Keywords:
Absolute quantification
Inductive coupling
Pseudo-signal
Metabolite content
Sample resistance
Coil loading

ABSTRACT

Conversion of MR signals into units of metabolite concentration requires a very high level of diligence to account for the numerous parameters and transformations that affect the proportionality between the quantity of excited nuclei in the acquisition volume and the integrated area of the corresponding peak in the spectrum. We describe a method that eases this burden with respect to the transformations that occur during and following data acquisition. The conceptual approach is similar to the ERETIC method, which uses a pre-calibrated, artificial reference signal as a calibration factor to accomplish the conversion. The distinguishing feature of our method is that the artificial signal is introduced strictly via induction, rather than radiation. We tested a prototype probe that includes a second RF coil rigidly positioned close to the receive coil so that there was constant mutual inductance between them. The artificial signal was transmitted through the second RF coil and acquired by the receive coil in parallel with the real signal. Our results demonstrate that the calibration factor is immune to changes in sample resistance. This is a key advantage because it removes the cumbersome requirement that coil loading conditions be the same for the calibration sample as for experimental samples. The method should be adaptable to human studies and could allow more practical and accurate quantification of metabolite content.

1. Introduction

A practical and robust method for converting signals into units of metabolite content would greatly improve the accuracy, information content, and utility of MR measurements. Quantification of metabolite content, a process often referred to as absolute quantification, requires accurate determination of the proportionality factor between the quantity of excited nuclei associated with that metabolite within the measurement volume and the integrated area of the corresponding spectral peak in the processed data. In general, a very high degree of diligence is required to account for all of the parameters that affect this calibration factor. As a result, nearly all MR results are presented in terms of arbitrary units or as ratios, which can be difficult to interpret and of limited clinical and experimental utility.

We have developed a method that eases the burden of the quantification process. Our approach utilizes a small RF coil (the injector coil) that couples inductively with the RF coil used for signal acquisition. The purpose of the injector coil is to stimulate a robust synthetic signal (the pseudo-signal) in the receiver coil at the same time that the real signal is acquired from the sample. The amplitude, frequency and linewidth of the pseudo-signal are first set relative to a real peak corresponding to a known metabolite concentration. The same pseudo-signal is then injected during subsequent measurements and used as a reference signal for converting the real signals into standard units of concentration.

The key innovation of this approach is that the pseudo-signal is introduced to the receiver coil via inductive coupling. Since this is also the mechanism by which the local B_1 field (B_{1m}) arising from excited nuclei in the sample couples with the receiver coil, any subsequent manipulations of the data have an equal effect on both signals. This makes the calibration factor immune to changes in coil loading conditions, receiver gain settings and data processing methods.

We have built and implemented a prototype probe and we have conducted in vitro experiments to verify that the pseudo-signal and the real signals are completely independent of each other—a necessity for accurate quantification—and that the ratio of the pseudo-signal and real signal is immune to variations in coil loading. Our approach could allow more practical and accurate quantification of metabolite content using non-invasive MR techniques.

2. Experimental

All experiments were conducted on a 4.7 T Bruker horizontal bore magnet equipped with a Varian Inova spectrometer and

* Corresponding author. Fax: +1 206 543 3495.
E-mail address: marro@u.washington.edu (K.I. Marro).
[1] These authors contributed equally to this work.

1090-7807/$ - see front matter © 2008 Published by Elsevier Inc.
doi:10.1016/j.jmr.2008.05.022

VNMR version 6.1. The pulse sequence and RF coil were modified to allow injection of a pseudo-signal during acquisition of the real signals, as described below. Before each measurement, the tune and match capacitors were adjusted to yield 50 Ω impedance, the B_o field was optimized by manually adjusting the shims, and the flip angle was set to maximize the real signal. The integrated areas of the spectral peaks generated by the real and pseudo-signals were determined using the Advanced Method for Accurate, Robust and Efficient Spectral (AMARES) time domain fitting algorithm [1] as included in the Java-based Magnetic Resonance User Interface (jMRUI) software package [2].

Signal excitation and acquisition were achieved using a 2 cm diameter surface coil. The experiments were specifically designed to avoid potential errors in quantification caused by the highly non-uniform B_1 field generated by the surface coil. This eliminated the need for spatial calibration measurements. A simple pulse-acquire sequence was used for all measurements and the repetition time was always much longer than the T_1 of the samples. This eliminated the need to compensate for differences in relaxation times for different samples.

2.1. Probe design

Our prototype probe consisted of a 2 cm diameter surface coil (C1 in Fig. 1) and a 1.5 mm diameter, 2-turn injector coil (C2), both formed from copper wire. C1 was tunable to both ^{1}H and ^{31}P frequencies, 200.4 and 81.2 MHz, respectively, and was operated in both transmit and receive modes. The injector coil was used solely to inject the pseudo-signal into the surface coil during data acquisition. To minimize coupling between the injector coil and the sample, C2 was oriented perpendicular to the plane defined by C1.

A straightforward circuit analysis provides insight into how the probe satisfies the key constraints described in Section 3. Fig. 2A shows the main components of the probe, the voltage source used to inject the reference signal, and the preamplifier used to acquire the signals as the components are used during signal acquisition.

As shown schematically in Circuit A of Fig. 2, the injector coil and the main RF coil were placed in close proximity to each other (1 mm separation between them) so there was mutual inductance, M, between them. The mutual inductance is defined as, $M = k(L_iL_c)^{1/2}$, where k is a scalar that depends on the geometric arrangement of the two coils. In our probe, the injector coil was rigidly mounted to the main RF coil so k was a constant. This is a key feature of the design because it ensures that M is a constant and, therefore, that the pseudo-signal remains in calibration when the probe is repositioned in the magnet to accommodate different samples. Any change in M during the course of the study would have been obvious because it would have required breaking the bonds holding the probe together.

As shown in Circuit B of Fig. 2, the elements comprising the voltage source and the injector coil can be replaced with an equivalent voltage source and resistor, e'_r and R'_r, respectively, where

$$e'_r = \frac{j\omega M}{R_r + R_i + j\omega L_i} e_r \quad R'_r = \frac{\omega^2 M^2}{R_r + R_i + j\omega L_i}. \tag{1}$$

The parameters on the right-hand sides of these two equations are constants determined by fixed physical characteristics of the hardware that do not change after the calibration session. By summing the voltage drops around the two loops in Circuit B, two simultaneous equations can be generated. These can be solved in order to determine the detected signal, V_p,

$$V_p = \frac{R_p}{D}(e_s + e'_r)$$
$$D = \left\{1 + \frac{C_t}{C_m} + j\omega C_t R_p\right\}\left\{R_s + R'_r + R_c + j\omega L_c + \frac{1}{j\omega C_t}\right\} - \frac{1}{j\omega C_t}. \tag{2}$$

Note that the sample-dependent variables, R_s, C_t, and C_m, are all in the denominator, D, and they act in equal proportion on the two terms in the numerator, e_s and e'_r. In this analysis, we have assumed a single value for the frequency, ω. In practice, the frequency for the injected signal, ω_r, will be deliberately set to a slightly different frequency from the metabolite frequency, ω_s, so that the peaks in the processed spectrum do not overlap. The difference between ω_r and ω_s, which is on the order of a few kilohertz, is much smaller than the resonant frequency, which is at least tens of megahertz, so this will introduce a negligible error into the analysis but it also allows the acquired signal to be divided into two components,

$$V_p = V_s(\omega_s) + V_r(\omega_r) \tag{3}$$

$$V_s(\omega_s) = \frac{R_p}{D} e_s(\omega_s)$$
$$V_r(\omega_r) = \frac{R_p}{D} e'_r(\omega_r)$$

where V_s arises from the sample and V_r is the voltage of the injected reference signal.

This analysis demonstrates that the calibration factor, $V_r(\omega_r)/V_s(\omega_s) = e'_r(\omega_r)/e_s(\omega_s)$, is independent of the sample-dependent parameters that affect coil loading so, after it is set during the calibration session, it remains constant.

2.2. Properties of the injector coil

The analysis above assumes that the only coupling mechanism between the injector circuit and C1 is inductive. The injector coil

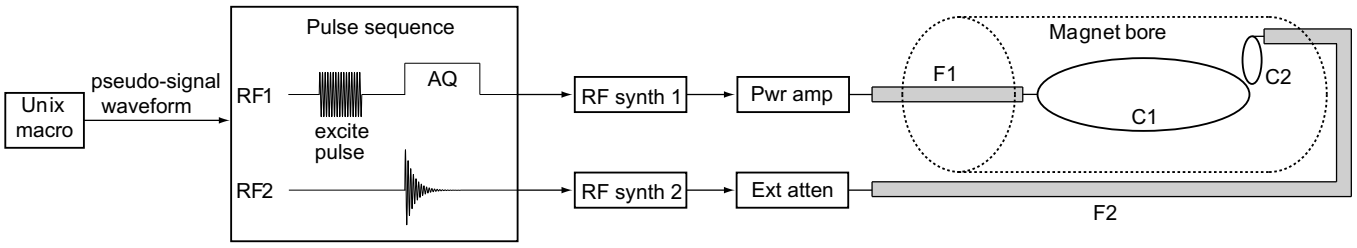

Fig. 1. This schematic depicts the key components required to implement the quantification protocol. Prior to execution of the pulse sequence, a Unix macro was used to create a digitized waveform describing the desired pseudo-signal. The pulse sequence read the waveform and sent it to the second RF channel (RF2). The pseudo-signal was transmitted through an RF synthesizer (RF synth 2) and passed through an external attenuator (Ext atten) before being fed through an RG-223 coaxial cable (F2) to the injector coil (C2). The diameter of C2 was much smaller than C1 and it was oriented perpendicular to the surface of the sample. To prevent cross talk between the two coaxial cables (F1 and F2), the distance between them was maximized by feeding them in through opposite ends of the magnet bore. During sequence execution, C1 was operated in transmit/receive mode while C2 was used only to transmit the pseudo-signal during the acquisition window (AQ). The main RF channel (RF1) and the components linking it to C1 were operated as they would be for a typical pulse sequence. We show a simple pulse-acquire sequence and a pseudo-FID but more sophisticated sequences and pseudo-signals can be implemented.

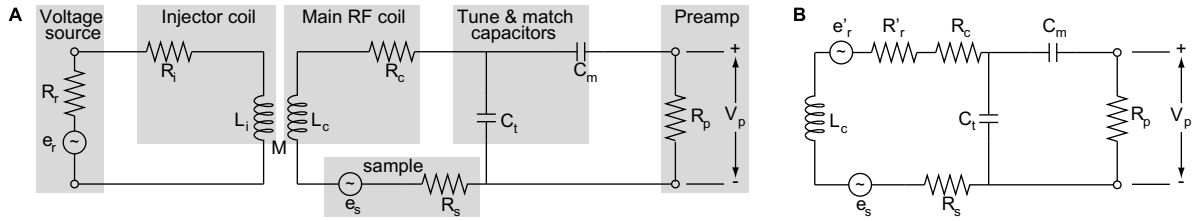

Fig. 2. Circuit A shows the main components of the hardware needed to implement the quantification method. The probe consists of the injector coil and the main RF coil. Each coil can be modeled as a fixed resistor and a fixed inductor, R_i and L_i for the injector coil and R_c and L_c for the main coil. Since these two coils are placed close together, there is mutual inductance, M, between them. Current around the injector coil loop is driven by the RF synthesizer and external attenuator (see Fig. 1). These can be modeled as a voltage source, e_r, and a fixed resistor, R_r. During signal acquisition, excited spins in the sample create a current around the main RF coil loop. The sample can be modeled as a voltage source, e_s and a resistive load, R_s. In general, R_s, and the tuning and matching capacitors, C_t, and C_m, are sample-dependent variables because, when the sample changes, R_s changes and C_t, and C_m must be adjusted so that the net impedance of the main RF coil loop is 50 Ω. The acquired signal arises from the current flowing through the fixed resistor, R_p, in the preamplifier, generating the voltage, V_p. In Circuit B, the components comprising the voltage source and the injector coil have been replaced with an equivalent voltage source, e'_r, and an equivalent resistor, R'_r, where these parameters are as defined in the text.

and the cable driving it must be designed so that reflected power and the formation of standing waves are negligible or else the injector circuit could act as an antenna and transmit a signal to C1 via radiation coupling. To minimize reflected power, a 50 Ω, non-magnetic resistor was included in series with the injector coil. The return losses at the ^{1}H and ^{31}P frequencies were 14.9 and 26.8 dB, respectively. The power reflection coefficients of the injector circuit and the main RF coil circuit were calculated using the values of resistance and reactance as measured at the BNC connectors on the coaxial driving cables (Table 1).

To further attenuate formation of standing waves, bazooka baluns [3] were placed on the coaxial driving cables (F1 and F2). Additional precautions against radiation coupling between the two cables included the use of RG-223 cable, which has two layers of double silver braid for shielding, and maximizing the separation distance between the cables by running them out opposite ends of the magnet bore, as shown in Fig. 1.

2.3. Pulse sequence modifications

Modifications to the pulse sequence were necessary in order to transmit the pseudo-signals during data acquisition. In all cases described in this study the pseudo-signals were designed to mimic FIDs. A UNIX-based macro was used to generate files containing digitized descriptions of the pseudo-signals in terms of amplitude and phase variations over time. Inputs to the macro were the duration (δ), linewidth (λ), frequency offset (ω), and number of points (N) desired in the pseudo-signal. The macro was executed prior to running the pulse sequence and the amplitude and phase data were stored in formats that were compatible with pulse sequence commands. The amplitude waveforms were calculated according to the following equation,

$$A_p(n) = A_{p,nom} \exp\left(\frac{-T_p(n)}{T_{2p}}\right) \quad (4)$$

where $n = 1{:}N$, $A_p(n)$ is the amplitude of the pseudo-signal at each digitized point; $A_{p,nom}$ is the nominal amplitude of the pseudo-signal, $T_p(n) = n\delta/N$; and $T_{2p} = 1/(\Pi\lambda)$. The frequency offset, relative to the RF transmitter frequency, was controlled by ramping the phase of the signal in the phase waveform file, providing a complex character to Eq. (4).

The pulse sequence subsequently accessed these files and transmitted the artificial FID waveforms through the second RF synthesizer (see Fig. 1) at the same time that the real signals were being acquired from the samples. The duration of the pseudo-signal was always set to be equal to the acquisition window used to acquire the real data and the number of points in the pseudo-signal corresponded to the block size. This ensured that, during the data acquisition window, the pseudo-signal evolved exactly like a real FID arising from the sample.

Table 1
Properties of the RF coils

Frequency (MHz)	Injector coil		Main RF coil	
	Impedance (Ω)	Reflection coefficient (%)	Impedance (Ω)	Reflection coefficient (%)
81.2 (^{31}P)	47.3 + j6.4	0.005	53.5 + j3.2	0.002
200.4 (^{1}H)	48.5 + j15.8	0.020	39.4 – j12.3	0.030

2.4. Tests to demonstrate that the real signal is not altered by the pseudo-signal

In vitro measurements were acquired at both ^{1}H and ^{31}P resonances from two different phantoms; one containing 5 M methanol and one containing 400 mM phosphoric acid (H_3PO_4) (SW = 5000 Hz, block size = 8k points, single acquisition, TR = 30 s). The DAC unit parameter, which controls the nominal amplitude of the pseudo-signal waveform ($A_{p,nom}$ in Eq. (4)), was increased from 100 to 1000 for the methanol measurements and from 0 to 2000 for the H_3PO_4 measurements. (Full range is from 0 to 4096.) This provided linear control of $A_{p,nom}$.

2.5. Tests to demonstrate that the pseudo-signal is not altered by the real signal

Measurements were obtained from six phantoms with varying methanol concentration while keeping $A_{p,nom}$ constant (TR = 30 s, SW = 5000, block size = 8k, 4 averages) The volumetrically determined methanol concentrations were 0, 2.5, 5.0, 7.4, 9.9, and 12.3 M.

2.6. Tests to demonstrate that the calibration factor is not affected by coil loading conditions

Measurements were acquired at both ^{1}H and ^{31}P resonances from two different phantoms to observe changes in the real and pseudo-signals under different coil loading conditions. The ^{1}H measurements were conducted on a water phantom, i.e., with no methanol, due to concerns over salt solubility in high methanol concentrations. The ^{1}H phantom was simply a 12 cm diameter bowl containing 250 cc of water resting directly on top of the 2 cm diameter surface coil. To vary the ionic strength and hence the effective resistance of the surface coil salt, (NaCl) was added to the water to form concentrations of 25, 50, 100, 150, and 200 mM.

The ^{31}P phantom was identical to the ^{1}H phantom except that a 1.2 cm diameter tube containing 5 cc of highly concentrated (2.9 M) H_3PO_4 was centered in the bowl, directly above and perpendicular to the surface coil. This provided a strong Pi signal but kept the solution well away from the surface coil and therefore minimized the coil loading effects caused by dissociation of the H_3PO_4 in water. A wide range of well-controlled coil loading conditions was then induced by varying the salt concentration in the surrounding saline solution to form concentrations of 0, 40, 80, 120, 160, and 200 mM.

2.7. In vitro quantification of metabolite concentration

To test the accuracy of the method when both coil loading and metabolite concentration vary, ^{31}P measurements were obtained from a series of phantoms with volumetrically determined concentrations of 60, 118, 176, 233, 291, 347, 404, 460, 515, and 570 mM H_3PO_4 (TR = 30 s, SW = 5000, block size = 8k, 4 averages). The following equation was used to calculate the H_3PO_4 concentration from the Pi peak [4],

$$C_m = C_{ref} \frac{A_m}{A_p} \frac{A_{p,ref}}{A_{m,ref}} \quad (5)$$

where C_m is the calculated metabolite concentration, C_{ref} is the independently measured metabolite concentration used during the calibration session, A_m and A_p are the areas of the metabolite and pseudo-signal peaks, respectively, $A_{m,ref}$ and $A_{p,ref}$ are the areas of the metabolite and pseudo-signal peaks, respectively, acquired during the calibration session. The measurements made at the highest H_3PO_4 concentration, and highest signal-to-noise ratio (SNR), were assigned as the calibration session.

3. Results

Fig. 3 shows sample spectra acquired from an H_3PO_4 phantom with and without injection of the pseudo-signal. In general, the amplitude and linewidth of the pseudo-signal can be set to approximate the real peak used for calibration. The frequency and phase can be set so that the pseudo-peak does not overlap with any real peaks. All of these parameters were easily controlled by pulse sequence variables. No significant increase in spectral noise due to injection of the pseudo-signal was observed in any of the measurements conducted in this study, indicating that the method can be implemented with no SNR penalty.

The method used to introduce the pseudo-signal must meet certain constraints in order to accomplish accurate and robust quantification. Our experiments were designed to examine three of these constraints:

1. That variations in the amplitude of the injected pseudo-signal do not change the magnitude of the real signal.
2. That variations in metabolite concentration do not change the magnitude of the pseudo-signal.
3. That the ratio of the real signal to the pseudo-signal is independent of coil loading conditions.

3.1. Variations in the amplitude of the injected pseudo-signal do not change the magnitude of the real signal

Fig. 4 shows the results of experiments designed to demonstrate that the amplitude of the pseudo-signal can be independently adjusted, as desired, without affecting the real signal. In Fig. 4A, the amplitude of the pseudo-signal increased linearly as the amplitude of the RF power supplied to the injector coil (C2) increased from 100 to 1000 DAC units, while the amplitude of the real ^{1}H signal, arising from a 5 M concentration of methanol, remained constant. Similar results were obtained at the ^{31}P resonance using a 400 mM sample of H_3PO_4 (Fig. 4B).

3.2. Variations in metabolite concentration do not change the magnitude of the pseudo-signal

Fig. 5 displays results from experiments in which we examined the behavior of the pseudo-signal during changes in the amplitude of the real signal. The amplitude of the real signal was changed by varying the concentration of methanol in an in vitro sample while keeping the amplifier power used to generate the pseudo-signal constant. As expected, the integrated area of the methanol signal increased linearly with concentration while the area of the pseudo-signal remained constant. The combined results in Figs. 4 and 5 demonstrate complete independence between the pseudo-signal and the real signal arising from the metabolite in the sample, a condition that must be met for accurate quantification of metabolite content.

3.3. The ratio of the real signal to the pseudo-signal is independent of coil loading conditions

The data in Fig. 6 show the changes in the real signal and the pseudo-signal over a wide range of coil loading conditions, which were induced by varying the salt concentration in a water phantom

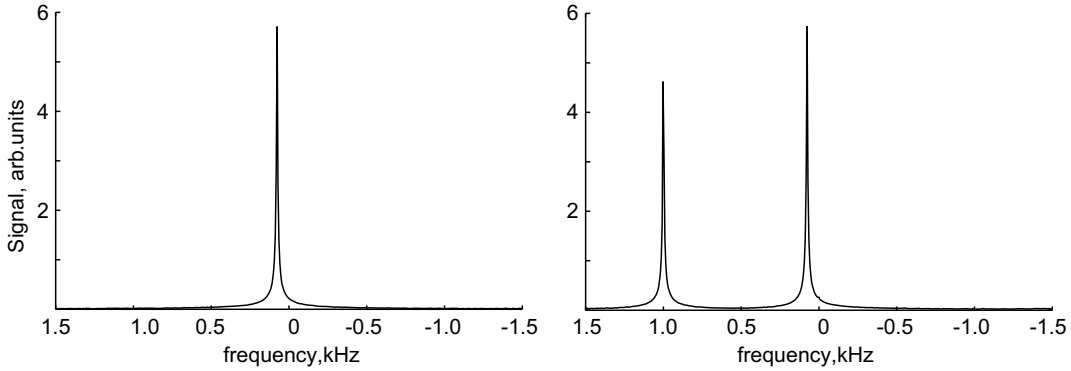

Fig. 3. The figures show typical ^{31}P spectra acquired from a phantom (2.9 M H_3PO_4 and 200 mM NaCl) with and without injection of the pseudo-signal. The amplitude, linewidth, phase, and frequency of the pseudo-signal can easily be set as desired by the user. Injection of the pseudo-signal does not alter the amplitude of real peaks (see Fig. 4) and does not introduce any significant noise. For these two spectra, the standard deviation of the signal measured between −1350 and −1450 Hz was essentially the same (2.368×10^{-3} without the pseudo-signal, 2.457×10^{-3} with the pseudo-signal).

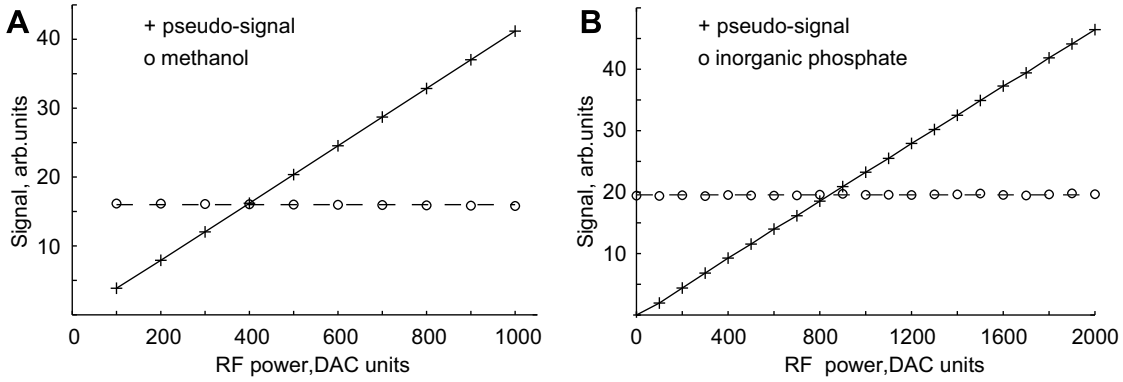

Fig. 4. (A) The integrated peak areas of the pseudo-signal and the real ^{1}H signal arising from the methyl group of methanol in a constant 5 M solution in water are shown as the RF power supplied to the injector coil was increased from 100 to 1000 DAC units. (Full scale is 0 to 4096 DAC units.) The pseudo-signal increased linearly with RF power while the methanol signal remained constant, indicating that the amplitude of the pseudo-signal can be set as desired without altering the real signal. (B) Similar results were obtained for the Pi signal from a constant 400 mM solution of H_3PO_4 as the RF power was increased from 0 to 2000 DAC units.

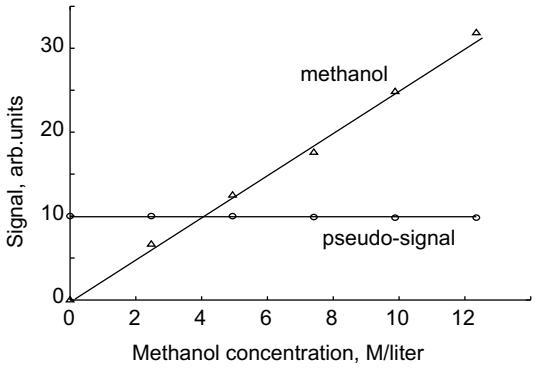

Fig. 5. In these experiments the concentration of methanol was increased from 0 to 12.3 M in six increments while the RF power used to generate the pseudo-signal ($A_{p,nom}$ in Eq. (4)) was held constant. The amplitude of the methanol signal increased linearly with methanol concentration but the amplitude of the pseudo-signal remained constant. These results demonstrate that the calibration factor, as determined by the amplitude of the pseudo-signal relative to a known metabolite concentration, remains constant when the metabolite concentration changes.

and an H_3PO_4 phantom. As salt concentration increased, the Q of the coil decreased and the duration of the excitation pulse required to maximize the signal increased. Both of these changes were caused by increased sample resistance (R_s) as the ionic strength of the solution increased. The increase in R_s, in turn, caused a substantial decrease in the integrated area of the real signals. The pseudo-signal was affected equally by R_s so that the ratio between the real signals and the pseudo-signals remained constant over the wide range of coil loading conditions tested. These results demonstrate that our method eliminates the requirement that coil loading conditions be identical when acquiring the reference and in vivo signals.

3.4. In vitro quantification of metabolite concentration

The results described above demonstrate that the calibration factor remains valid when either concentration or coil loading conditions change. The results in Fig. 7 demonstrate that accurate quantification can be achieved when these parameters are changed simultaneously. Increasing H_3PO_4 concentration caused increases in R_s. This increase in coil loading is evident from the approximately 35% drop in the integrated area of the pseudo-signal and the 50% increase in pw_{max} between the lowest and highest phosphoric acid concentrations. Coil loading conditions also affected the area of the Pi peak, causing it to deviate from the line of identity at higher H_3PO_4 concentrations. However, the H_3PO_4 concentrations, as calculated from Eq. (5) were all very close to the line of identity, indicating that the calibration factor, determined at the highest H_3PO_4 concentration, remained valid over these wide ranges of concentration and coil loading conditions.

4. Discussion

The many factors involved in converting MR signals into units of metabolite content can be divided into two groups. The first group includes transformations that occur during and following data acquisition and determine the proportionality between the magnitude of the B_{1m} field generated within the acquisition volume by a given metabolite concentration and the integrated area of the peak in the processed spectrum. This group includes:

- *Coil loading:* Electromagnetic coupling between the RF coil and the sample determines the effective resistance of the coil, which in turn determines the amplitude of the current generated in the coil by B_{1m}. Loading can vary between subjects and can change during the course of a measurement session due to motion.
- *Receiver gain stability:* The gain of the RF amplifier can drift over time. Correction for drift requires separate calibration measurements.
- *Data processing algorithm:* Many different data processing algorithms are available to convert the raw MR data to spectra and then to perform the integration of the peaks. The various algorithms can yield different peak areas depending on the details of implementation.

Our approach eases the burden of the quantification process with respect to this group of parameters. Accurate quantification still requires due diligence to compensate for, or minimize the effects of, the second group of parameters, which includes processes that occur prior to data acquisition and affect the magnitude of B_{1m}. Among other factors this group includes:

- T_1, T_2, *TR and TE:* Relaxation times vary between metabolites and the pulse sequence, repetition time, and echo time can have a substantial effect on the signal amplitudes.
- B_1 *field homogeneity:* Local variations in the amplitude of the B_1 field generated by the RF coil can affect the flip angle, reception sensitivity, and integrity of volume selection and therefore the amplitude of the acquired signal.
- *Frequency response of the RF pulse:* Non-uniform excitation of different chemical species can occur if the frequency response of

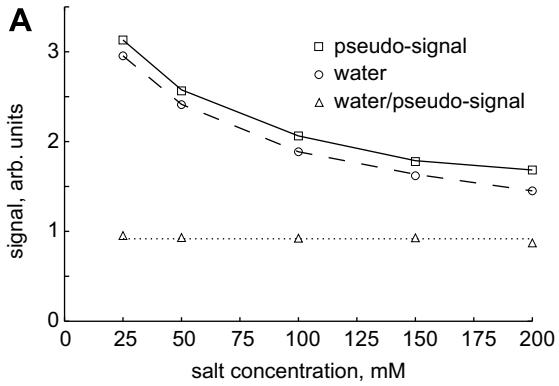

[NaCl] mM	Q	pw_{max} μsec
25	568	47
50	376	52
100	228	62
150	167	67
200	142	73

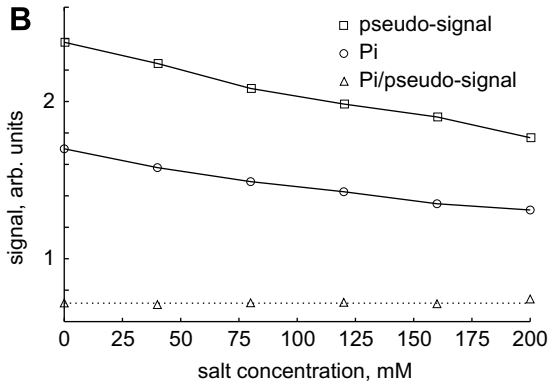

[NaCl] mM	Q	pw_{max} μsec
0	958	46.0
40	796	50.0
80	724	52.5
120	647	55.0
160	591	57.5
200	545	60.0

Fig. 6. These data demonstrate that the calibration factor, once determined at a known concentration, does not change due to variations in coil loading conditions. The data in (A) were acquired from a water phantom and the data in (B) were acquired from a phantom containing H_3PO_4. In both phantoms, the salt concentration was varied to alter coil loading conditions. The tables show that, as the salt concentration increased, the *Q* of the coil decreased and the nominal pulse width increased, reflecting large increases in sample resistance (R_s in Fig. 2). Graph A shows that the water signal decreased by more than 50%, from about 2.9 to less than 1.5 (arbitrary units) as the salt concentration increased. The pseudo-signal decreased proportionately so that the ratio (water/pseudo-signal) remained essentially constant with a mean value of 0.91 (dotted line in the graph). Similar results were obtained from the Pi phantom. Both the pseudo-signal and the Pi signal decreased as salt concentration increased but the ratio of the two signals remained essentially constant at about 0.71. This demonstrates that a single calibration measurement will allow accurate quantification over a very large range of coil loading conditions.

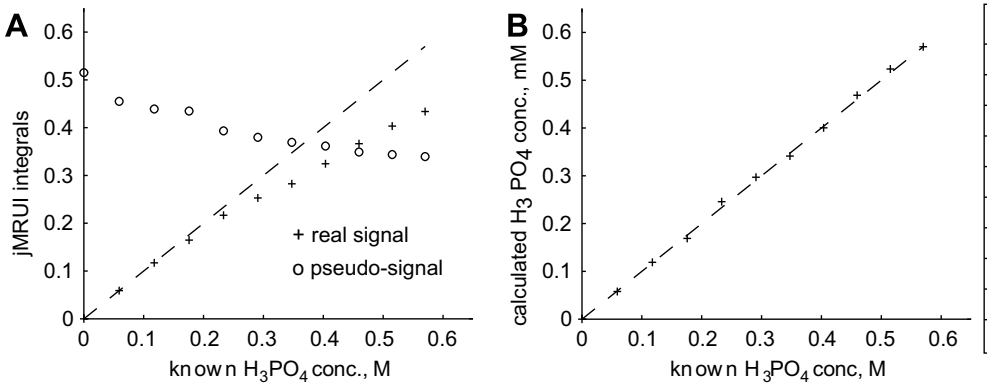

$[H_3PO_4]$ mM	pw_{max} μsec
60	27
118	30
176	33
233	36
291	36
347	38
404	38
460	39
515	41
570	41

Fig. 7. Graph A shows the integrated areas of both the Pi signal and the pseudo-signal as a function of H_3PO_4 concentration. As H_3PO_4 concentration increased, the ion concentration in the sample increased and so did the sample resistance, R_s. The changes in R_s increased the load on the coil used to acquire the signal, resulting in a non-linear relationship between H_3PO_4 concentration and the area of the Pi signal, as indicated by the deviation from the straight (dashed) line at the higher concentrations. The changes in coil loading had an equivalent affect on the pseudo-signal, causing it to decrease in amplitude at higher concentrations. Graph B shows the H_3PO_4 concentrations as calculated using Eq. (5). The calculated concentrations are all very close to the line of identity (dashed line), indicating that the calibration factor remains constant despite changes in both metabolite concentration and coil loading conditions. Measurements of *Q* for the receiver coil were not obtained but the accompanying table shows that pw_{max} increased from 27 to 41 μs over the full range of H_3PO_4 concentrations. The increases in pw_{max} reflect decreases in *Q* that were comparable to those in Fig. 6.

the pulse is not constant over the frequency range covering all the nuclei of interest.

- *Flip angle deviations:* Quantitative errors can result if the actual flip angles differ from the nominal/desired flip angle. Sensitivity to these deviations is pulse sequence dependent.
- *MR visibility:* The available signal depends on binding conditions and, in some cases, orientational effects in the tissue [5].
- *Magnetization transfer effects:* Diffusion-driven exchange between pools of nuclei can affect the available signal if off resonance pulses are employed (e.g. for fat suppression, water suppression or outer volume suppression).

A large number of papers have been published addressing the second group of parameters and it is beyond the scope of this paper to summarize or improve upon them.

The general algorithm most often used to convert MR spectra to units of metabolite content is to acquire a reference signal from a sample with a known concentration, establish the calibration factor between the reference metabolite concentration and the integrated area of the reference peak, and then use that calibration factor to convert in vivo peaks of interest into units of concentration [6–8]. Most implementations of this algorithm can be divided into two groups, depending on whether the reference signal is obtained from within the subject (internal reference) or from a phantom placed outside the subject but within the sensitive volume of the RF coil (external reference). The calibration factor can also be determined using the principle of reciprocity [9].

The internal reference method uses either an in vivo metabolite signal [10,11] or the in vivo water signal as the reference standard [12–16]. The main advantage of this approach is that it does not require separate measurements to calibrate the reference signal. This eliminates problems due to differences in coil loading in the calibration and in vivo sessions. An inherent assumption behind this approach is that the reference metabolite or tissue water concentration is accurately known and remains stable during the course of the measurement. The physiological water content in the central nervous system is relatively stable in healthy subjects and appears to remain fairly constant during edema [17] but it can vary substantially due to disease [18,19]. There is no reliable reference metabolite that allows this method to be broadly applied to ^{31}P measurements.

With external reference methods, a vial containing a known concentration of an MR-visible substance is placed outside the subject but within the sensitive volume of the RF coil. A spectrum from the external reference standard is recorded during [20,21] or after data [22–25] acquisition of the in vivo data. This method does not rely on assumptions regarding tissue composition and can yield high SNR data. However, the external reference standard is susceptible to RF field inhomogeneities, inaccuracies of transmitter gain settings [26] and potential mismatch of loading conditions if the external reference standard is acquired in a separate session from the in vivo data.

Metabolite quantification can also be achieved without the use of a physical sample to establish the required calibration factor. Instead, the RF coil voltage needed to produce a known flip angle in the measurement volume is determined. The principle of reciprocity [9] is then used to calculate the magnitude of the B_1 field—and therefore the quantity of nuclei—that must be present in the measurement volume in order to generate the peak areas observed in the in vivo spectra. Each quantification method has specific weaknesses that limit practical utility. As a result, none of these methods has achieved widespread clinical acceptance.

The ERETIC (Electronic REference To access In vivo Concentrations) method is an innovative approach to metabolite quantification that was proposed by Barantin et al. [27]. They showed that a calibrated synthetic signal could be acquired simultaneously with the in vivo signals and used as a reference for quantification. The artificial ERETIC signal can be provided using either a broad band antenna [27,28] or the second coil in a high-resolution MR probe [29–31]. High-resolution MR probes can only be used with samples that are small enough to fit within the required shielding that must be placed around the probe. When an antenna is used, the amplitude of the pseudo-signal depends not only on the power supplied to the antenna but also on the physical size and location of all RF reflectors and absorbers in the vicinity. This problem is commonly encountered in high frequency radio applications, where the strength of the received signal is known to be affected by standing wave reflections from nearby objects. It is feasible, using a high degree of diligence, to control for some of the factors that affect reflection and absorption of the broadcast RF signal, such as antenna position, sample size and position, cable lengths and positions, and position of other objects in the magnet room. But highly predictable signal reception is not possible when large objects of variable shapes, such as humans, are present in the bore of the magnet, except under tightly controlled and limiting conditions.

The use of an artificially injected pseudo-signal to quantify metabolite content offers several advantages over the internal and external reference methods. The user has complete freedom to set the amplitude, frequency, phase, and linewidth of the reference peak as desired. The frequency can be set to a convenient location, within the acquisition bandwidth but not overlapping the in vivo peaks. To minimize differential effects of data processing techniques, the amplitude and linewidth can be set to approximate in vivo peaks. The method can be applied to any nucleus and time consuming searches and preparations of calibration samples can be eliminated. Lastly, the electronically injected reference signal is readily available, eliminating the need to maintain stable biochemical samples for use as external references.

When implementing this approach, great care must be taken to avoid damaging the receive circuitry of the system. The amplitude of the injected signal must be limited so that the current it generates in the receive coil is comparable to that generated by the nuclei within the acquisition volume. We achieved this by passing the pseudo-signal generated by the pulse sequence through an external 30 dB attenuator and bypassing the power amplifier (see Fig. 1). The pulse sequence modifications required to inject the pseudo-signal during acquisition of the in vivo signal may not be trivial. All MR instrument manufacturers include safety features in the system software and hardware to ensure that direct RF pulses from a source amplifier are not introduced during the acquisition phase of the pulse sequence, when they could damage the extremely sensitive receiver components of the instruments. The effort required to bypass these safety features will vary between different magnet systems and is generally eased in systems that allow homonuclear decoupling during acquisition.

4.1. Probe design

The key innovation that we are introducing is the use of inductive coupling to inject the pseudo-signal. Robust implementation of this approach requires a probe that is designed to:

- Provide efficient and constant mutual inductance between the injector and receive coils.
- Minimize inductive coupling between the injector coil and the sample.
- Minimize radiation coupling between the injector and receive circuits.

Our probe design incorporated several features to meet these constraints. The diameter of our injector coil, 1.5 mm, was more than an order of magnitude smaller than the diameter of the surface coil (2 cm) used to excite and acquire the signals. This small diameter and the location of the injector coil—on the opposite side of the surface coil, relative to the sample—ensured that inductive coupling between the injector coil and the sample was negligible because the magnetic field falls off with the square of the coil diameter. The small size of the injector coil also minimized the load it placed on the transmit/receive coil so that no blocking circuit was necessary to prevent coupling when the latter was operated in transmit mode.

The injector coil was fixed in position with a separation distance of 1 mm between it and the surface coil. Fixed positioning of the injector coil was an important feature of the design because we

noted that even very small changes (<1 mm) in position, relative to the surface coil, altered the mutual inductance between the two coils and destroyed the calibration factor.

The probe included a 50 Ω resistor in the injector coil circuit, to optimize matching with the transmitter amplifier, and bazooka baluns [3] on the driving cable to suppress common mode currents on the shield. These precautions alone were not sufficient to eliminate radiation coupling between the injector coil cable and the surface coil cable. In our initial experiments we used two RG-58 cables, one for the injector coil and one for surface coil, laid parallel to each other, approximately 15 cm apart, and running out the same end of the magnet bore. With this arrangement there was substantial radiation coupling between the two cables. This coupling mechanism completely bypasses the surface coil, so the amplitude of the pseudo-signal in the processed spectrum does not change with coil loading conditions. Empirical evidence for coupling between the cables was that the integrated area of the pseudo-signal remained essentially constant as the salt concentration increased in experiments similar to those of Fig. 6 (data not shown). To eliminate radiation coupling, we switched to RG-223 cable, which has two layers of double silver braid for shielding, and we maximized the separation distance between the two cables by running them out opposite ends of the magnet bore, as shown schematically in Fig. 1.

We note that, since we were using a surface coil to excite and receive the real signals, all our measurements were conducted using a simple pulse-acquire sequence and phantoms that were specifically designed to eliminate potential errors in quantification that could arise due to the highly non-uniform B_1 field created by the coil. In order to acquire spatially localized measurements with this probe, spatial calibration measurements would generally be needed to account for the non-uniform field. Implementation of the method using a well-designed volume coil would eliminate the need for spatial calibration measurements provided that all the measurements were acquired within the homogenous region of the coil.

4.2. Independence of the real and pseudo-signals

Accurate and robust quantification requires that there be complete independence between the processed pseudo-signal and the real signal. This independence is generally not in question for in vivo signals; if the concentration of a single metabolite changes, only the peak corresponding to that metabolite changes in the acquired spectrum. It is not obvious that this feature holds true for an artificially injected signal. The circuit analysis accompanying Fig. 2 predicts this independence and the results presented in Figs. 4 and 5 validate the prediction.

Comparison of spectra with and without the presence of the pseudo-signal, such as those shown in Fig. 3, confirmed that the noise level in the spectra is essentially constant. Fig. 4 shows that the amplitude of the real signal also remains constant. These results demonstrate that the method can be implemented with no detrimental effect on the SNR of the measurements.

4.3. Immunity to coil loading conditions

An important advantage of using inductive coupling to inject the pseudo-signal is that it is also the mechanism by which B_{1m} couples with the receive coil. As we show in the circuit analysis accompanying Fig. 2, all subsequent manipulations of the data have an equal effect on the real and pseudo-signals. If coil loading conditions change, either between experiments or during the course of a single experiment, the current produced in the receive coil by the excited nuclei and the current produced by the injected pseudo-signal will be scaled up or down in the same proportion. Therefore the ratio of the integrated area of the injected peak to the area of an in vivo peak will stay constant (see Fig. 6), preserving the calibration and making quantification robust.

The data in Fig. 6 demonstrate that the calibration factor remains robust when coil loading is the only parameter that changes. The data in Fig. 7 demonstrate that accurate quantification can be achieved when both coil loading and metabolite concentration change. An important difference between these two experiments is in the properties of the solutes used. Methanol is an extremely weak acid. Its hydroxyl proton exchanges with water protons but no ions are produced so changes in methanol concentration do not change the electric field that interacts with the RF coil. In contrast, H_3PO_4 is an extremely strong acid. When it dissolves in water it dissociates and produces ions. As the H_3PO_4 concentration increased in Fig. 7, the ion concentration increased, altering the electric field within the sample and increasing R_s, the effective resistance of the RF coil used to acquire the MR signal. The increase in R_s caused pw_{max} to increase by more than 50% as the H_3PO_4 concentration increased from 60 to 570 mM. The increased resistance spoiled the otherwise linear relationship between H_3PO_4 concentration and the integrated area of the Pi signal. However, since induction was the mechanism of coupling for both B_{1m} and the injector coil, the changes in coil loading affected the Pi signal and the pseudo-signal in the same proportion. Eq. (5) could then be used to accurately determine the H_3PO_4 concentration without the need to compensate for coil loading changes.

Use of inductive coupling to inject the pseudo-signal eliminates the substantial burden imposed if coil loading must be identical for the calibration and in vivo measurements, as is required for most other absolute quantification methods. In order to match coil loading conditions, it is necessary to adjust the electrolyte content of the calibration phantom, using an iterative trial and error process. Our modeling and experimental results demonstrate that this tedious, time consuming and error-prone process can be avoided when a properly designed injector coil is used to create a stable reference signal. This approach makes the quantification process independent of the properties of the sample so that, once the calibration factor is set during the calibration session, it remains constant.

5. Conclusions

We have designed and built a prototype probe that uses inductive coupling to inject a stable pseudo-signal into the receive coil. The pseudo-signal can be acquired in parallel with the real signal arising from the sample. The system design minimized radiation coupling and ensured that the dominant mechanism of coupling between the injector circuit and the receive circuit was induction between the two coils.

The general protocol for converting peak amplitudes into units of metabolite content would begin with a calibration measurement on a sample with a known concentration of an MR-visible metabolite. The calibration session could be conducted on a suitable phantom or on an in vivo sample, if there were an internal reference peak for which the metabolite content were accurately known. The amplitude and linewidth of the pseudo-peak would be adjusted to approximate the amplitude of the real reference peak. The frequency of the pseudo-peak would be set to a region of the spectrum where no real peaks appear. These measurements would establish the calibration factor between the amplitude of B_{1m} and the concentration of the reference metabolite. The identical parameters would be used to inject the pseudo-signal in subsequent in vitro or in vivo measurements and the calibration factor would remain valid, provided that all the variables that affect the amplitude of B_{1m} (see Section 4) were accurately accounted for.

Our results demonstrate that the amplitude of the real signal and the pseudo-signal are completely independent and that the ratio of the two peaks is immune to changes in coil loading conditions. Once the pseudo-signal is properly calibrated against a known concentration, the calibration factor should remain stable, provided the physical arrangement of the coils is unaltered. We chose to integrate our injector coil with a surface coil but the principles involved are general and should transfer directly to other receive coils. The method should be adaptable to human studies and could allow more practical and accurate quantification of metabolite content.

References

[1] L. Vanhamme, A. van den Boogaart, S. Van Huffel, Improved method for accurate and efficient quantification of MRS data with use of prior knowledge, J. Magn. Reson. 129 (1) (1997) 35–43.

[2] A. Naressi, C. Couturier, J.M. Devos, M. Janssen, C. Mangeat, R. de Beer, D. Graveron-Demilly, Java-based graphical user interface for the MRUI quantitation package, MAGMA 12 (2–3) (2001) 141–152.

[3] G. Amvame-Nze, A.J.M. Soares, F. da Costa Silva, Analysis and tests of the new cylindrical dipole antenna structure with a bazooka balun. Foz do Iguacu, Brazil, 2003.

[4] V. Silvestre, S. Goupry, M. Trieweiler, R. Robins, S. Akoka, Determination of substrate and product concentrations in lactic acid bacterial fermentations by proton NMR using the ERETIC method, Anal. Chem. 73 (2001) 1862–1868.

[5] I. Asllani, E. Shankland, T. Pratum, M. Kushmerick, Anisotropic orientation of lactate in skeletal muscle observed by dipolar coupling in (1)H NMR spectroscopy, J. Magn. Reson. 139 (2) (1999) 213–224.

[6] O. Henriksen, In vivo quantitation of metabolite concentrations in the brain by means of proton MRS, NMR Biomed. 8 (4) (1995) 139–148.

[7] J.F. Jansen, W.H. Backes, K. Nicolay, M.E. Kooi, ^{1}H NMR spectroscopy of the brain: absolute quantification of metabolites, Radiology 240 (2) (2006) 318–332.

[8] R. Kreis, Quantitative localized ^{1}H NMR spectroscopy for clinical use, J. Prog. NMR Spectrosc. 31 (1997) 155–195.

[9] D.I. Hoult, R.E. Richards, The signal-to-noise ratio of the nuclear magnetic resonance experiment, J. Magn. Reson. 24 (1) (1976) 71–85.

[10] L. Chang, T. Ernst, C. Tornatore, H. Aronow, R. Melchor, I. Walot, E. Singer, M. Cornford, Metabolite abnormalities in progressive multifocal leukoencephalopathy by proton magnetic resonance spectroscopy, Neurology 48 (4) (1997) 836–845.

[11] V.P. Mathews, P.B. Barker, S.J. Blackband, J.C. Chatham, R.N. Bryan, Cerebral metabolites in patients with acute and subacute strokes: concentrations determined by quantitative proton MR spectroscopy, AJR Am. J. Roentgenol. 165 (3) (1995) 633–638.

[12] R. Kreis, T. Ernst, B.D. Ross, Absolute quantitation of water and metabolites in the human brain: 2. Metabolite concentrations, J. Magn. Reson. B 102 (1) (1993) 9–19.

[13] E.R. Danielsen, O. Henriksen, Absolute quantitative proton NMR spectroscopy based on the amplitude of the local water suppression pulse. Quantification of brain water and metabolites, NMR Biomed. 7 (7) (1994) 311–318.

[14] W. Dreher, D. Leibfritz, New method for the simultaneous detection of metabolites and water in localized in vivo ^{1}H nuclear magnetic resonance spectroscopy, Magn. Reson. Med. 54 (1) (2005) 190–195.

[15] K.R. Thulborn, J.J.H. Ackerman, Absolute molar concentrations by NMR in inhomogeneous B1. A scheme for analysis of in vivo metabolites, J. Magn. Reson. 55 (3) (1983) 357–371.

[16] P.S. Tofts, The noninvasive measurement of absolute metabolite concentrations in vivo using surface-coil NMR spectroscopy, J. Magn. Reson. 80 (1) (1988) 84–95.

[17] R. Kreis, E. Arcinue, T. Ernst, T. Shonk, R. Flores, B. Ross, Hypoxic encephalopathy after near-drowning studies by quantitative ^{1}H magnetic resonance spectroscopy, J. Clin. Invest. 97 (5) (1996) 1142–1154.

[18] G. Helms, Volume correction for edema in single-volume proton MR spectroscopy of contrast-enhancing multiple sclerosis lesions, Magn. Reson. Med. 46 (2) (2001) 256–263.

[19] I. Mader, W. Roser, L. Kappos, G. Hagberg, J. Seelig, E.W. Radue, W. Steinbrich, Serial proton MR spectroscopy of contrast-enhancing multiple sclerosis plaques: absolute metabolic values over 2 years during a clinical pharmacological study, AJNR Am. J. Neuroradiol. 21 (7) (2000) 1220–1227.

[20] R. Buchli, P. Boesiger, Comparison of methods for the determination of absolute metabolite concentrations in human muscles by ^{31}P MRS, Magn. Reson. Med. 30 (5) (1993) 552–558.

[21] C.A. Husted, J.H. Duijn, G.B. Matson, A.A. Maudsley, M.W. Weiner, Molar quantitation of in vivo proton metabolites in human brain with 3D magnetic resonance spectroscopic imaging, Magn. Reson. Imaging 12 (4) (1994) 661–667.

[22] E. De Bisschop, R. Luypaert, G. Annaert, J. Coremans, M. Osteaux, Absolute quantification of ^{31}P liver metabolites in rat using an external reference and a surface spoiling magnetic field gradient, NMR Biomed. 5 (6) (1992) 341–346.

[23] J.K. Gard, G.M. Kichura, J.J.H. Ackerman, J.D. Eisenberg, J.J. Billadello, B.E. Sobel, R.W. Gross, Quantitative ^{31}P nuclear magnetic resonance analysis of metabolite concentrations in Langendorff-perfused rabbit hearts, Biophys. J. 48 (5) (1985) 803–813.

[24] H.P. Hetherington, D.D. Spencer, J.T. Vaughan, J.W. Pan, Quantitative ^{31}P spectroscopic imaging of human brain at 4 Tesla: assessment of gray and white matter differences of phosphocreatine and ATP, Magn. Reson. Med. 45 (1) (2001) 46–52.

[25] A. Subramanian, A. Gupta, S. Saxena, A. Gupta, J. Kumar, A. Nigam, R. Kumar, S.K. Mandal, R. Roy, Proton MR CSF analysis and a new software as predictors for the differentiation of meningitis in children, NMR Biomed. 18 (4) (2005) 213–225.

[26] R. Kreis, T. Ernst, B.D. Ross, Development of the human brain: in vivo quantification of metabolite and water content with proton magnetic resonance spectroscopy, Magn. Reson. Med. 30 (4) (1993) 424–437.

[27] L. Barantin, A. Le Pape, S. Akoka, A new method for absolute quantitation of MRS metabolites, Magn. Reson. Med. 38 (2) (1997) 179–182.

[28] S. Akoka, M. Trierweiler, Improvement of the ERETIC method by digital synthesis of the signal and addition of a broadband antenna inside the NMR probe, Instrum. Sci. Technol. 30 (1) (2002) 21–29.

[29] S. Akoka, L. Barantin, M. Trierweiler, Concentration measurement by proton NMR using the ERETIC method, Anal. Chem. 71 (13) (1999) 2554–2557.

[30] V. Silvestre, S. Goupry, M. Trierweiler, R. Robins, S. Akoka, Determination of substrate and product concentrations in lactic acid bacterial fermentations by proton NMR using the ERETIC method, Anal. Chem. 73 (8) (2001) 1862–1868.

[31] V. Molinier, B. Fenet, J. Fitremann, A. Bouchu, Y. Queneau, Concentration measurements of sucrose and sugar surfactants solutions by using the ^{1}H NMR ERETIC method, Carbohydr. Res. 341 (11) (2006) 1890–1895.